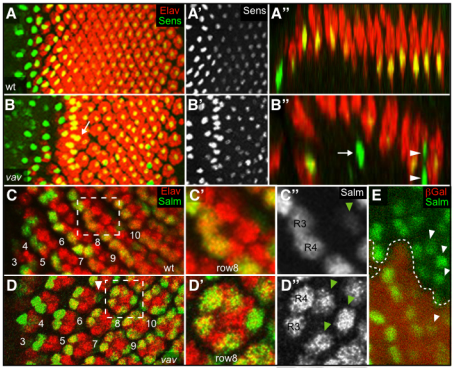

Figure S1. Extra R7 cells are recruited precociously to forming ommatidia in *vav* mutant larval eye discs.

Third-instar larval eye discs are oriented with anterior towards the left. **(A-B)** Co-staining with antibodies against Elav (red) and Sens (R8, green) reveals that ectopic R8s are recruited in *vav* discs (arrow). Z projection images. **(A)** Wild-type. **(B)** *Vav* disc. **(A″-B″)** Re-slicing the stack of images revealed that extra R8s actually fail to differentiate further as neurons as seen by the lack of Elav staining, and fail to recruit more R cells as there are isolated. Extra R8s are located underneath (arrow) or in between (arrowheads) ommatidia. **(C-D)** Discs from salm-lacZ larvae stained with anti-Elav antibody (red) to mark neurons and anti-β-gal antibody (green) to mark R3/R4. Rows of ommatidial differentiation are indicated. **(C′, C″, D′, D″)** Enlargements of the regions outlined in C and D. **(C′, D′)** Merged channels. **(C″, D″)** Salm staining (green channel). **(C)** In *salm-lacZ*/+ larvae, Salm expression is restricted to only two cells, the R3 and R4 until row 7. Salm expression starts to be detected in three cells in row 8, with a weak expression in the putative R7 (arrowhead). **(D)** In *vav; salm-lacZ*/+ larvae, Salm expression is restricted to R3/R4 until row 5 only. White arrowhead indicates a putative R7 in row 6. In row 8, Salm is strongly expressed in five cells, with three putative R7s, also supported by the cell position in the cluster (arrowheads). **(E)** *vav*FRT19A/*arm-lacZ*FRT19A; *eyflp*/+ larval eye disc stained with β-gal (red) to identify vav mutant tissue (no β-gal) and Salm to visualized R3, R4 and R7. The limit of the clone is highlighted by the dotted line. Five Salm-positive cells are present in vav mutant ommatidia, whereas wild-type ommatidia display only three positive cells on the same row, showing extra R cell recruitment in the vav mutant cells. Putative R7s are indicated by arrowheads.

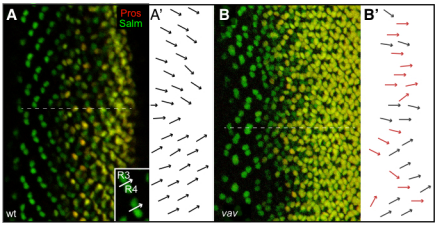

Figure S2. Ommatidia rotation defects in *vav* mutant larval eye discs.

(A-B) Third-instar larval eye discs are oriented with anterior towards the left. At the time R3 and R4 are specified, the developing ommatidial cluster rotate 90° in the dorsal and ventral halves of the eye on each side of the dorsoventral midline, also called the equator (represented by a dotted line). Anti-Pros antibody (red) and anti-β-gal antibody (green) to mark R3/R4 were used. **(A)** *Salm-lacZ* larva. Ommatidia close to the morphogenetic furrow (to the left) are perpendicular to the equator. Around row 6, ommatidia have rotated 45°, and in the posterior part of the disc, the 90° rotation is almost complete. Tracing an arrow between R3 and R4 gives the orientation of a single ommatidium (inset). **(A')** Arrows were traced on top of the picture in A, and the picture was removed to highlight the orientation of ommatidia in the first rows of differentiation. Correct orientations are indicated by black arrows **(B)**. *Vav; salm-lacZ* larva. In addition to the extra cells phenotype, many ommatidia display rotation defects. **(B')** Mis-rotated ommatidia are indicated by red arrows.

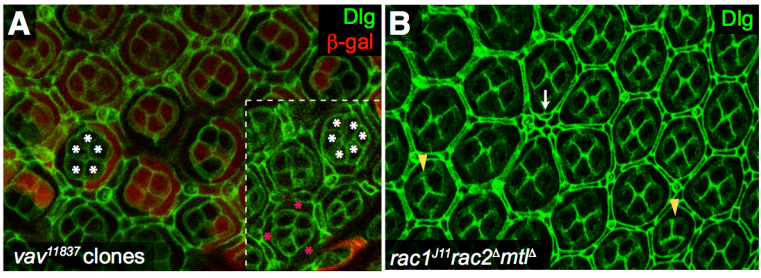

Figure S3. Triple *rac* cells do not display the same phenotypes as *vav* in the eye.

(A) *Vav11837*FRT19A/*arm-lacZ*FRT19A; *eyflp*/+ pupae were dissected and retinae stained with anti-Dlg antibody (green) and anti-β-gal (red) antibody. *Vav11837* allele displays the same phenotypes as the *vav1, vav2* and *vav3* alleles. *Vav* mutant clones are revealed by the absence of β-gal staining. The extra CC phenotype is highlighted by white stars and the extra 1° phenotype by pink stars. The image in the inset comes from a different retina. **(B)** Retina almost entirely mutant for *rac1, rac2,* and *mtl* were generated. As opposed to *vav* mutant, no ommatidia with extra CCs nor 1°s are found. A few ommatidia even displayed the opposite phenotype with less CCs (yellow arrowheads, 5.7%, n= 450 from 3 retinae) . Only extra interommatidial cells (arrow) are detected, although the phenotype was less frequent and milder than in *vav* retina.

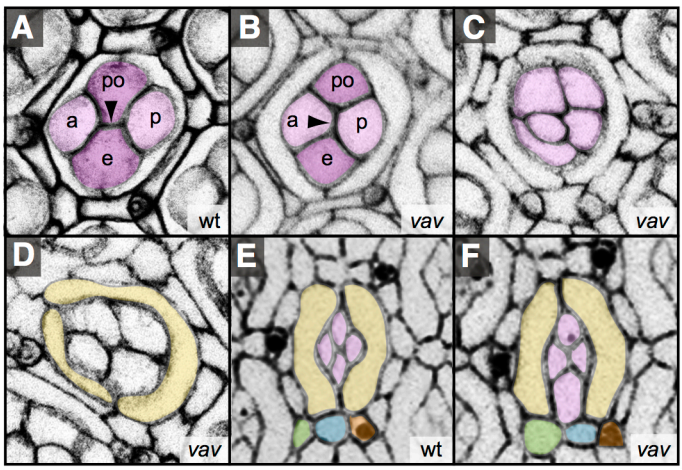

Figure S4. *Vav* mutant phenotypes related to putative junctional or adhesion defects at the retinal apical surface.

Apical views of 48 h APF retinae stained with anti-Dlg antibody to visualize septate junctions **(A-D)** or anti-Armadillo antibody to visualize adherens junctions **(E-F)**. The different cell types are pseudo-coloured for easier identification: CCs in pink, 1°s in yellow, 2°s and 3°s in blue and green respectively, bristles in brown. **(A)** In wild-type, polar (po) and equatorial (e) CCs are in contact at the centre of the cluster, whereas anterior (a) and posterior (p) CCs are separated. In *vav* tissue, defects in the CC cluster include orientation of CC junctions (64% of ommatidia) **(B)** and CCs not arranged in an energetically stable manner that is normally used to maximise adhesion between cells (37% of the ommatidia) **(C)**. **(D)** 1°s of different sizes (23% of ommatidia). **(E)** In wild-type, the two 1°s are forming a collar around the CC cluster. **(F)** In *vav* ommatidia, defects in junctional integrity leads to an opening between the two 1°s, so the CC cluster enters in contact with the IPC (Open 1° phenotype, 7% of ommatidia).

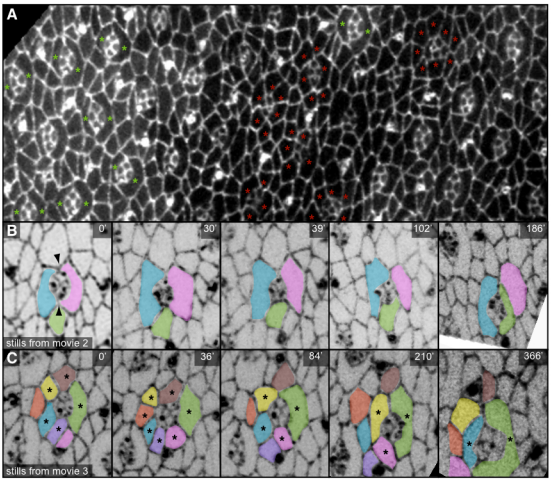

Figure S5. Unstable 1°:1° junctions cause cells to be highly dynamics and delay cell recruitment in *vav* mutants.

(A) Pupa of the following genotype was selected: *vavFRT*19A/*ubiGFPeyFlp122*FRT19A; *DE-cadherin:GFP*/+. Adherens junctions are marked by the DE-cadherin: GFP. *Vav* cells are identified by the lack of ubi-GFP. At the time wild-type ommatidia have recruited the two 1°s that enwrap the CC cluster (green stars), *vav* ommatidia are still surrounded by three to eight 1°-candidates (red stars). **(B-C)** Live imaging of *vav* ommatidia. Cells that are finally selected as 1°s are pseudo-coloured in blue and green for better clarity. **(B)** *vav* cells from a clonal region, showing that an established contact between two 1°s can be lost (at 30′). The 1°-like cell in pink that has adopted the typical elongated shape of 1°s is finally displaced by the 3°-like cell in green that changes its shape when it reaches the position to become a 1°. **(C)** *vav* cells are highly dynamics and compete to become 1°s. Cells in direct contact with the CC cluster are identified by black stars, showing that cells that are separated from the CC cluster can re-enter in contact with it (5 cells in contact at 0′ and 7 cells in contact at 36′). The yellow 1°-like elongated cell (at 210′) is displaced by the blue cell (366′) although the latest had totally lost contact with the CC cluster.

Supplementary Material Movie 1. Dynamics of wild type ommatidia assembly shown in Fig. 5A.

Live imaging of wild-type development on *DE-cadherin:GFP* pupa. Eyes were imaged at 2 min intervals. Primary pigment cell formation shows that once two 1°-like establish a contact, a junction is formed and maintained.

Supplementary Material Movie 2. Dynamics of the *vav* phenotype shown in Fig. S5B.

Live imaging of primary pigment cell formation defect in a *vav* mutant clonal region from *vav*FRT19A/*ubiGFPeyFlp*^{122}FRT19A; *DE-cadherin:GFP*/+ pupae. At the beginning of the movie, 1° selection seems to have occurred as two 1°-like cells with their typical elongated shape surround the CC cluster. However, an invading cell from the IPC is able to completely displace a previously established 1°-like cell from the CC cluster it was contacting, disrupting the 1°:1° junction, so the first pre-1° is moved to the interommatidial space. Eyes were imaged at 3 min intervals.

Supplementary Material Movie 3. Dynamics of the *vav* phenotype shown in Fig. S5C.

Cell competition for the 1° niche in a *vav mutant clonal region*. Cells surrounding the CC cluster are excessively motile and more than two cells compete during hours to become 1°s. Some of them initially contact the CCs, are displaced by adjacent cells exhibiting 1°-like behaviour, and then re-enter in contact with the CCs. One of these cells is eventually selected as the 1°. Eyes were imaged at 3 min intervals.

Supplementary Material Movie 4. Dynamics of the three 1°s phenotype shown in Fig. 5B.

Live imaging of *vav* mutant development in a clonal region. Three cells compete for the 1° niche. Two 1°-like establish and loose contact several times but a third cell finally stays in the middle leading to the recruitment of three 1°s around the CC cluster. Eyes were imaged at 3 min intervals.

Supplementary Material Movie 5. Dynamics of the open 1° phenotype shown in Fig. 5C.

Live imaging of *vav* mutant development in a clonal region. Two 1°s had established junctions but one of the junctions is lost after several hours. As a consequence, the CC cluster enters in contact with the interommatidial cells. Eyes were imaged at 3 min intervals.

Supplementary Material Movie 1

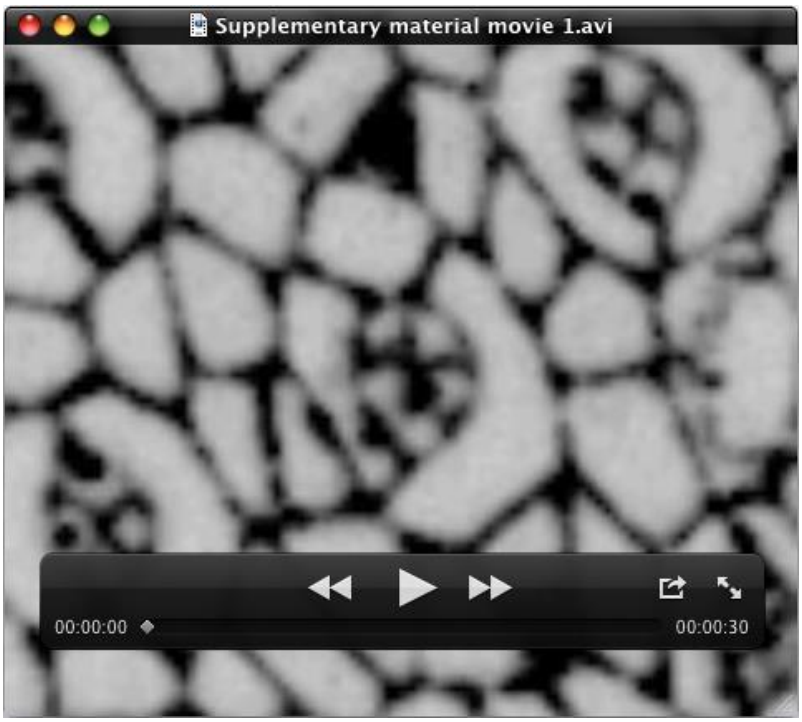

Supplementary Material Movie 2

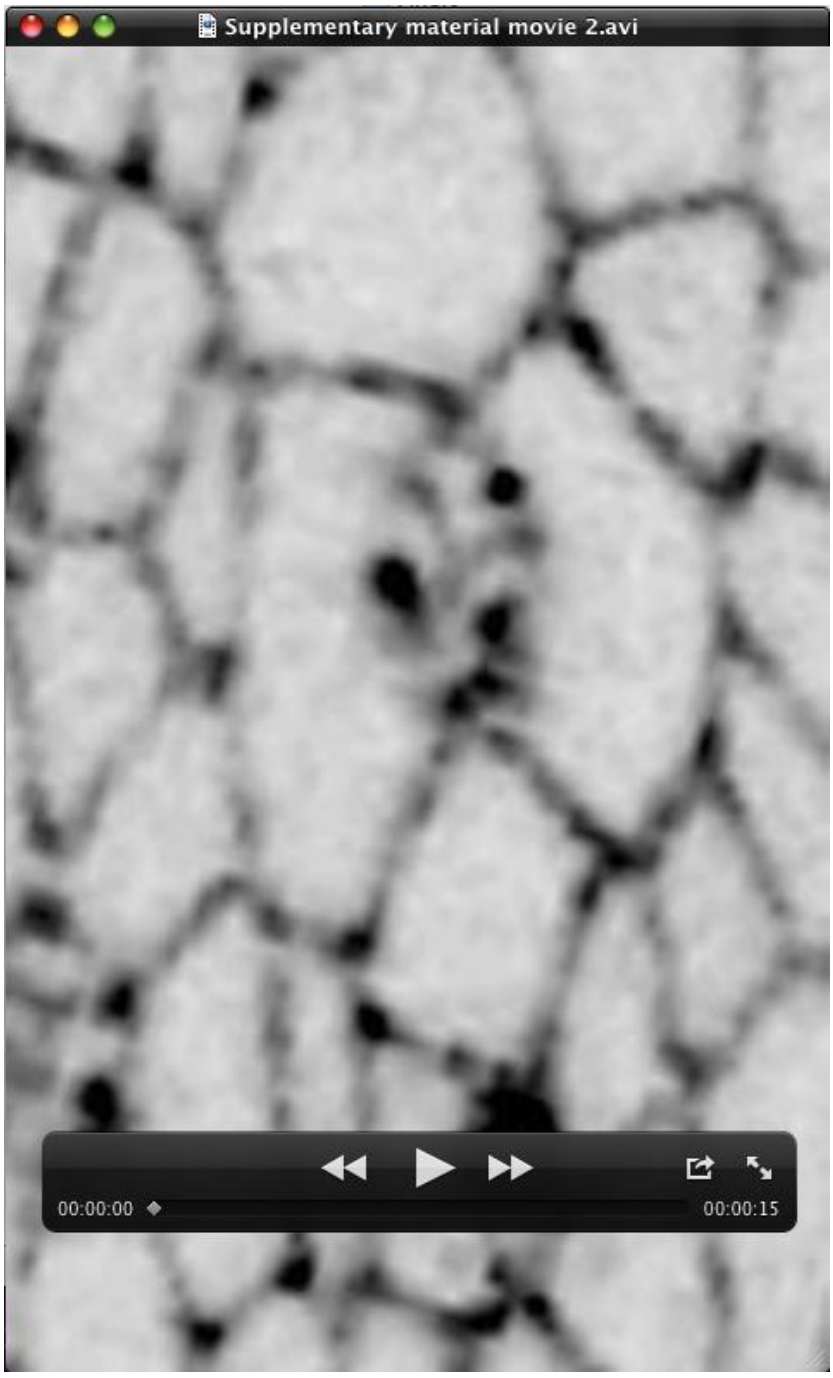

Supplementary Material Movie 3

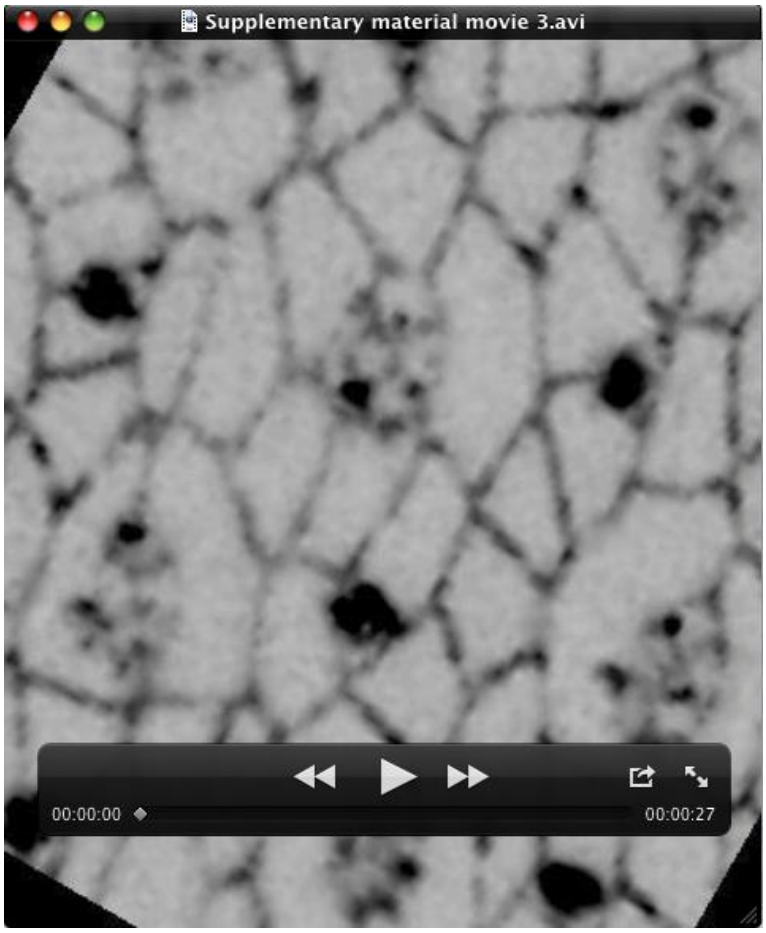

Supplementary Material Movie 4

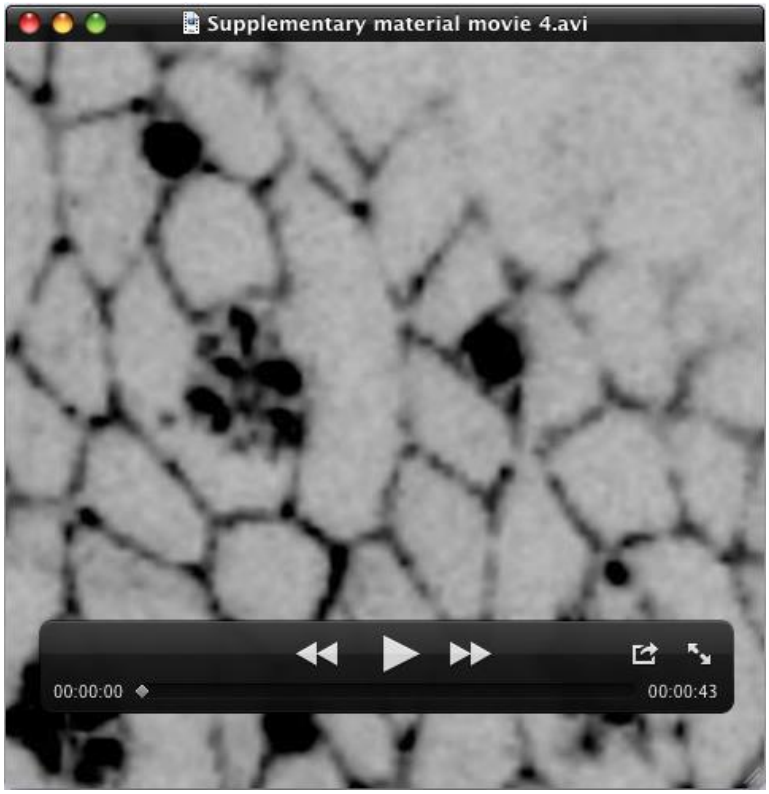

Supplementary Material Movie 5